INDIAN JOURNAL OF SCIENCE AND TECHNOLOGY

RESEARCH ARTICLE

Extraction and Characterization of Bismarck Palm Fibres

N Raja[1*], **S Raju**[2]

1 Research Scholar, Department of Manufacturing Engineering, Faculty of Engineering and Technology, Annamalai University, Annamalainagar, 608002, Tamil Nadu, India
2 Professor, Department of Manufacturing Engineering, Faculty of Engineering and Technology, Annamalai University, Annamalainagar, 608002, Tamil Nadu, India

OPEN ACCESS

Received: 29-09-2022

Accepted: 28-11-2022

Published: 24-12-2022

Citation: Raja N, Raju S (2022) Extraction and Characterization of Bismarck Palm Fibres. Indian Journal of Science and Technology 15(47): 2680-2689. https://doi.org/10.17485/IJST/v15i47.1624

* **Corresponding author**.

nvjrs1989@gmail.com

Funding: None

Competing Interests: None

Published By Indian Society for Education and Environment (iSee)

ISSN
Print: 0974-6846
Electronic: 0974-5645

Abstract

Objectives: A novel natural cellulose bismarck palm fibre (BPF) has been discovered and extracted from the leaf stalk of its tree. Physical, chemical, mechanical, and thermal characterizations have been conducted in this current study. **Methods:** A water retting method was employed for the extraction of BPFs. The diameter of BPF was assessed using an optical microscope image analyzer. A single fibre tensile test method was employed to calculate the tensile strength of BPF. The thermal behaviour of BPF was evaluated using thermo gravimetric analysis (TGA). A scanning electron microscope was utilized to evaluate the surface morphological structure of the BPF. **Findings:** The BPF has a fibre fineness of 819 denier, a mean diameter of 0.3636 mm, a density of 0.98 g/cc, cellulose content of 70.71%, hemi cellulose of 34.89%, lignin of 12.88%, wax of 0.30%, ash of 2.13 %, moisture of 10.80 %, pectin of 3.08 %, a mean breaking tensile strength of 904 MPa, mean breaking elongation of 6.4 %, and Young's modulus of 28.6 GPa, respectively. It is evident that the thermal analysis of BPF was thermally sustainable up to 268 °C. The results ensure that the BPF is the anticipated reinforcement of fibre-reinforced composite materials. SEM images revealed that cross section of BPF sample and rugged surface along the length of the fibre. **Novelty:** The higher cellulose percentage content of BPF samples has significantly shown better mechanical behaviour and thermal stability. This characterization evidenced that it is an outstanding alternative natural cellulose fibre for Eleusine indica grass fibres, Saccharum Bengalense fibres, Leucas Aspera fibres, Catharanthus roseus fibres, and Tridax procumbens fibres and also for synthetic fibres.

Keywords: Bismarck palm fibre; Natural cellulose fibre; Extraction; Characterization; Tensile strength

1 Introduction

Due to environmental pollution and the depletion of fossil fuels, all manufacturing industries have started replacing petroleum-based materials with natural-based materials to produce eco-friendly products. Natural fibre-reinforced composites are widely used for various applications to reduce emissions of greenhouse gases [(1)].

Environmental friendly and sustainable materials are gaining prominence in many engineering fields owing to their excellent strength-to-weight ratio, less cost, renewable, degradable, less energy required for processing, abundant in nature, non-toxic, and recyclability. The properties of natural fibres are affected by the cultivation process, environmental conditions, and extraction process [(2)]. The banyan tree root fibre demonstrated excellent resistance to fungal and bacterial development, which is unusual in natural fibres. As a result, they can be used in personal hygiene products like sanitary napkins, baby diapers, sanitary pads, face masks and so on [(3)]. The different extraction methods of natural cellulose fibres were evaluated, such as dew retting, water retting, and mechanical retting. Mechanical methods are extensively used in high-volume fibre extraction. A significant amount of fibre with a consistent diameter can be removed more quickly using mechanical methods, which are more expensive than the other two methods [(4)].

The researchers extracted and examined the characterization of Ficus Religiosa Root Fibre (FRRF). Because there was significantly more cellulose (55.58%), the FRRF had good mechanical and thermal properties [(5)]. The possibility of using Shwetark fibres, which are derived from the stems of plants, as polymeric reinforcement was investigated by the authors. The outcome demonstrates the feasibility of Shwetark fibres in replacing synthetic fibres [(6)]. The epoxy composites were made using Ziziphus mauritiana fibres taken from the novel Ziziphus Mauritiana plants. The findings demonstrate that the strength of the alkali-treated fibre-reinforced composites had a higher performance level than untreated fibre-reinforced composites [(7)]. The physical, chemical, mechanical, thermal, and morphological behaviour of chemically modified and unmodified Pennisetum Orientale grass (PO) fibre was examined. Based on the test results, chemically treated PO fibres had a cellulose content of 65.1% and reduced moisture and amorphous content [(8)]. The natural fibre was obtained from the Furcraea foetida plant using the water retting process. The possibility of fibre being converted into yarn for textile applications was examined using the results of fibre characterization. The findings indicate that plant fibre from Furcraea foetida may be used as a possible replacement material for textile applications [(9)].

The mechanical characteristics of several chemically treated sugar palm fibres (SPF) were investigated. The findings showed that silane-treated SPF-reinforced polyurethane composites outperform other treated SPF-reinforced polymer composites in terms of mechanical characteristics. As observed, modified SPFs have a great chance of replacing synthetic glass fibres [(10)]. This research aims to extract and characterize BPF in terms of its physical, chemical, mechanical, and thermal properties. Until now, BPFs had not been extensively characterized to assess their potential to replace synthetic fibre in polymer matrix composite reinforcement. The findings of this study can now be used by scientists, engineers, academicians, and researchers for further research.

2 Methodology

2.1 Extraction of BPFs

Bismarck palm trees are native to Madagascar. Bismarckia (bismarck palm trees) is the scientific name for a genus of flowering palm family plants. The genus is named after Otto von Bismarck, who was the first chancellor of the German Empire. The image of the Bismarck palm tree is shown in Figure 1 (a). BPFs were derived from the leaf stalk of the Bismarck palm tree, and the leaf stalks were cut down from locally available Bismarck palm trees. The leaves were removed from the stalks, and the thorns on the outside edges had been shaved. The skin of the leaf stalks was peeled off and cut into strips after being immersed in fresh running water for four weeks. After that, a hammer is used to lightly press the wet leaf stalks to separate the entangled fibre bundles. The fibres were then separated by hand. The fibres had a fleshy material stuck to the surface, which was removed with a wet cloth and dried in the sun to remove the moisture in the fibres. Figure 1 (b) shows extracted and dried BPFs.

2.2 Physical Characterization

Characterization methods are more important when selecting natural cellulose fibres to serve as reinforcement in composites made of polymeric matrix.

2.2.1 Fibre Fineness

The fibres were maintained at a temperature of 21 °C for an entire day, standard temperature, and 65% relative humidity before being tested. The cut and weigh method (SITRA/CP/01-2015) was used to determine fibre fineness. The quality of fibre is significantly influenced by its fineness. The denier, a textile measurement unit used for measuring fibre fineness, is denoted by the symbol ”den”. The number of fibres present in the cross-section of yarn of a given thickness is determined by fibre fineness. The yarn cross section must contain at least 30 fibres.

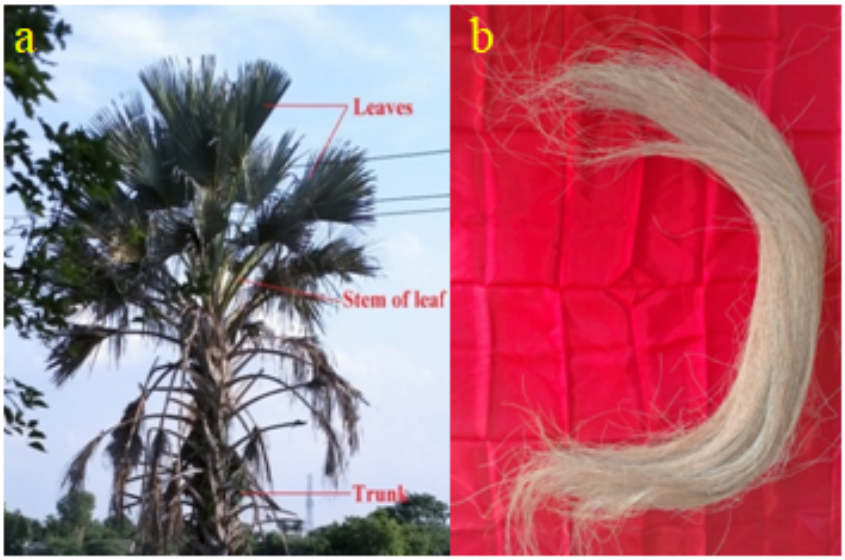

Fig 1. (a) Bismarck palm tree and (b) Extracted bismarck palm fibre

2.2.2 Fibre Diameter

An optical microscope was utilised to determine the diameter of BPF with a magnification of 100X. Figure 2 depicts the optical microscopic image of the measured diameter of individual Bismarck palm fibre. Because the diameter varies over the length of the fibres, measurements were made randomly at three different locations. Then, the mean diameter was determined after measuring ten samples of single fibres.

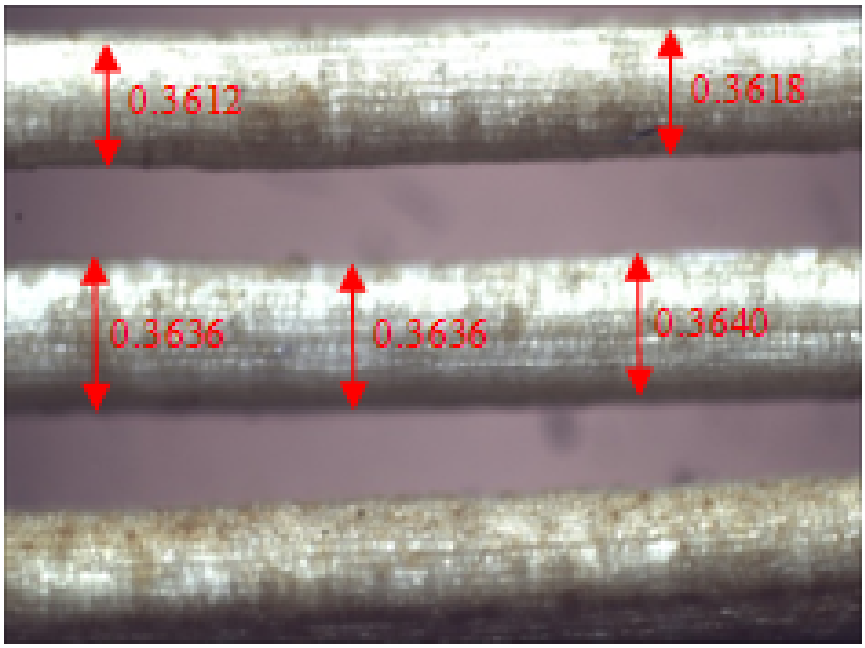

Fig 2. Optical microscopic image of BPF

2.2.3 Fibre Density

As shown in Equation (1), the density of the BPF was calculated by dividing its mass by volume. The container's volume and weight were first determined. Equation (2) was used to calculate the volume of the container. Then, m_2 was recorded as the container's initial weight. The BPFs were then ground into powder using a grinding machine. The container was then filled with powdered fibres. After that, the final weight of the container was recorded as m_1.

$$Density = \frac{mass\ (m_1 - m_2)}{volume} \frac{g}{cm^3} \tag{1}$$

$$Volume = height\ \times width\ \times depth\ cm^3 \tag{2}$$

2.3 Chemical Characterization

Cellulose, hemicellulose, lignin, waxes, ashes, moisture and pectin are the major components of natural fibres. SITRA/TC/FCC/01, SITRA/TC/FCC/02, and SITRA/TC/GT/09 standards were used to determine cellulose, lignin, and wax content. IS 199 standard was employed to compute the ash and moisture content present in the BPF fibres.

2.4 XRD Analysis

The extracted BPF structure was analysed using an X-ray diffractometer in accordance with ASTM D5187-91R02 standard. At 40 kV and 30 mA, the XRD was carried out using Cu Ka radiation (λ = 0.1542 nm). Data were gathered in step-scan mode throughout the range of 10° to 80°. The fibre crystallinity (%) was calculated using Equation (3).

$$Cristallinity\ (\%) = \frac{A_C}{(A_C + A_N)} \times 100 \tag{3}$$

Where A_C = Area under the crystalline peak and A_N = Area under the amorphous peak

The Scherrer's Equation (4) was used to determine the crystallite size of fibre.

$$Cristallite\ Size(nm) = \frac{K.\lambda}{\beta cos\theta} \tag{4}$$

Where K = Scherrer constant (0.9 rad.A^{-2}), λ= X-ray wavelength (0.1542 nm), β= Full width at half maximum (radians), and θ = Peak position (radians).

2.5 FTIR Analysis

The chemical composition of the BPF was examined using Fourier transform infrared (FTIR) spectroscopy in accordance with the ASTM E168 standard. The fibre was ground into a powder and combined with analytical-grade potassium bromide (KBr) before being compressed into a disc for measuring. The FTIR spectra were measured using 32 scans in the transmittance mode from 4000 to 400 cm^{-1}.

2.6 Mechanical Characterization

2.6.1 Single Fibre Tensile Test

The tensile strength of BPF was assessed utilising a universal testing machine (Make: Zwick Roell, Germany, Model: ProLine Z100, Year: 2015) universal testing machine in accordance with ASTM D3822. During testing, a crosshead speed of 1 mm/min was applied to a gauge length of 50 mm. A total of twenty-five samples were tested, and the results were recorded. Before testing, both ends of each fibre sample must be sealed with epoxy resin. The samples of prepared specimens for single-fibre tensile testing are shown in Figure 5 (a).

2.7 Thermal Characterization

The thermal characterization of the BPF was estimated employing a Simultaneous Thermal Analyzer (Make: NETZSCH India Pvt. Ltd., Model: STA 449 F3 JUPITER, Year: 2010) device. The TGA analysis plays a vital role in examining the thermal stability of natural fibre constituents because it needs to consider the operating temperature range of composite materials made of similar fibres. TGA experiments were carried out in atmospheric conditions with nitrogen from ambient temperature to 1000 °C at permanent heating. Gas flow rates were 20 degrees Celsius per minute and 40 millilitres per minute, respectively[11].

2.8 Microstructure Analysis

SEM (Make: JEOL India Pvt. Ltd., Model: IT200, Year: 2012) was employed to examine the longitudinal surface and cross-section view of extracted BPFs. A thin coating of gold was applied to the samples before SEM analysis utilizing a plasma sputtering device to prevent the charging effect. The SEM images were taken at different magnification levels with a 20 kV potential for accelerating electron beams.

3 Results and Discussions

3.1 Physical Characterization

BPF has an average diameter of 0.3636 mm, fibre fineness of 819 deniers, and fibre density of 0.98 g/cc. Table 1 shows the physical properties of BPF. The diameter of natural fibre varies over its total length due to changes in the environment and the conditions under which it is growing [12]. BPF has less density because of the hollow tubular nature of the fibres. The BPF density is 61% lower than the E-Glass fibre density (2.54 g/cc). The low density of BPF allows for greater flexibility in the fabricating composites made of polymeric matrices.

Table 1. Physical Characterization of BPFs

Fibre	Density (g/cc)	Diameter (mm)	Fibre Fineness (Denier)
BPF	0.98	0.2206 – 0.4527	819

3.2 Chemical Characterization

Table 2 shows the chemical composition of BPF compared with other natural fibres. Fibre properties are influenced by their chemical composition. Cellulose, lignin, and hemicellulose are the primary constituents of natural cellulosic fibres. The percentage of cellulose in BPF is 70.71 %. BPF has higher cellulose content than recently identified fibres, including Leucas Aspera, Tridax procumbens, Saccharum bengalense, Catharanthus roseus, and Eleusine indica. Greater cellulose content will result in better mechanical and thermal stability of the material. The assessed lignin value of BPF is 12.88 %, which is less than that of Catharanthus roseus fibre. Therefore, resistance to brittle failure increases as lignin content decreases.

Table 2. BPF Chemical Composition Comparison with other Natural CelluloseFibres

Fibre Name	Cellulose (%)	Lignin (%)	Wax (%)	Ash (%)	Moisture (%)	Pectin (%)	Hemi Cellulose (%)	Reference
BPF	70.71	12.88	0.30	2.13	10.80	3.08	34.89	Current study
Leucas Aspera	50.7	9.7	-	-	11.31	-	13.2	[13]
Tridax Procumbens	32	3	0.71	-	11.2	-	6.8	[14]
Saccharum Bengalense	53.45	11.7	1.30	5.6	2.1	-	31.45	[15]
Catharanthus roseus	47.3	15.1	2.3	-	8.3	-	9.1	[16]
Eleusine indica grass	61.3	11.12	2.9	2.5	5.6	-	14.7	[17]

3.3 Results of XRD Analysis

The X-ray diffraction plot of an extracted BPF is presented in Figure 3. The crystalline peaks, crystallinity and crystallite size are given in Table 3. The crystallised peak was observed at 22.66° on the BPF XRD plot. One important crystalline structure factor is the percentage of cellulose crystallinity. Increased crystallisation causes a decrease in the flexibility of the fibre and an increase in its rigidity. Compared to the previously discovered and characterised natural cellulose fibres, the BPF possessed a higher crystallinity (65.93%). This might be due to the presence of lesser non-cellulosic substances like hemicellulose and lignin, which have amorphous structures, and more crystalline cellulose. The great tenacity and improvement of the mechanical

properties of the relevant composites may have resulted from their high crystallinity. The crystal size of the BPF was 5.22 nm. This smaller crystal size made the BPF more chemically reactive and water-soluble, which might improve the dyeing of these fibres [18].

Table 3. Crystalline peak, Crystallinity and Crystal size of BPF compared with other Natural Cellulose Fibres

Fibre Name	Crystalline peak 2θ (°)	Crystallinity (%)	Crystal size (nm)	Reference
BPF	22.66	65.93	5.22	Current study
Tridax Procumbens	22.34	40.85	38.2	[14]
Yucca fibre	22.36	55.92	3.12	[18]

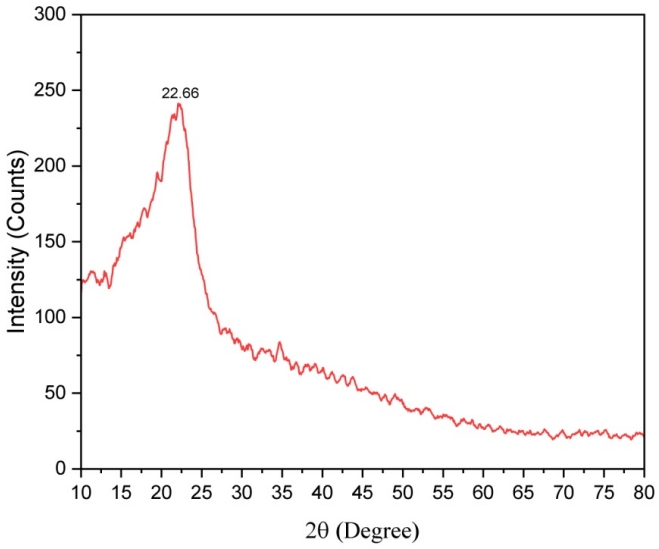

Fig 3. X- ray diffraction plot of the BPF

3.4 Results of FTIR Analysis

Figure 4 shows the Fourier transform infrared spectrum of the derived BPF. Six distinct peaks in the FTIR spectra of BPF were visible at 3429, 2924, 1640, 1384, 1034 and 619 cm^{-1}. The O-H stretching and bending vibration, which was the hydrogen-bonded hydroxyl (OH) group of cellulose and absorbed water, was said to be the cause of the peak at 3429 cm^{-1}. The C-H symmetric and asymmetric stretching were said to be responsible for the peaks at 2924 cm^{-1}. The C = C aromatic ring and C-H vibration of lignin were associated with the peak at 1640 cm^{-1}, whereas the C-H deformation of cellulose and lignin was associated with the peak at 1384 cm^{-1}. In addition, a peak at 1034 cm^{-1} shows the existence of the C–H rocking vibration in cellulose [18].

3.5 Mechanical Characterization

Figure 5 (b) shows the fractured specimen samples after single-fibre tensile testing. The mean tensile strength, Young's modulus, and percentage of breaking elongation of BPFs were 904 MPa, 28.6 GPa and 6.4 %, respectively. The results of the calculated tensile properties are tabulated in Table 4. In general, the tensile strength, Young's modulus, and percentage of breaking elongation of cellulose fibres rise as the cellulose content increases. The growing environmental conditions have an impact on the physical and mechanical characteristics of natural cellulose fibres.

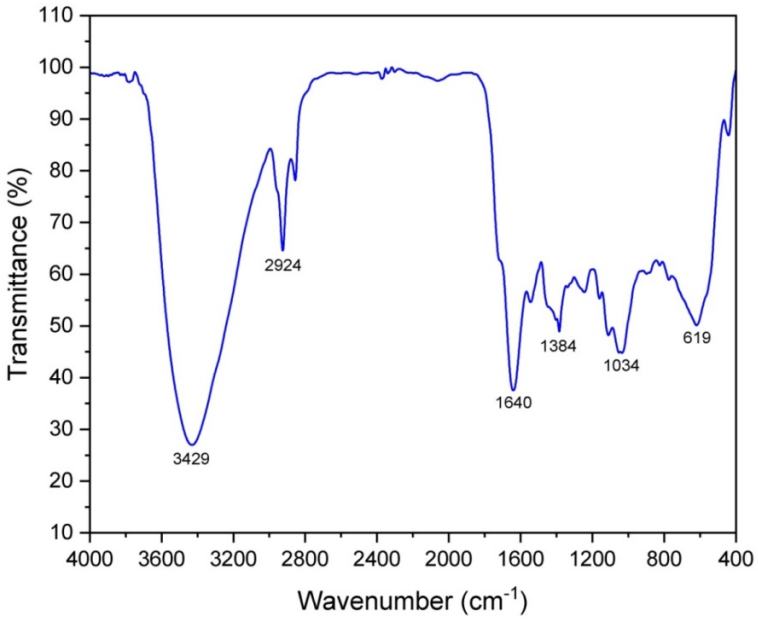

Fig 4. The FTIR spectrum of the extracted BPF

Table 4. Tensile Properties of BPF compared with other Natural Cellulose Fibres

Single Fibre Tensile Test	Mean Tensile Strength (MPa)	Mean Young's Modulus (GPa)	Mean Breaking Elongation (%)	Reference
BPF	904	28.6	6.4	Current study
Eleusine indica grass fibre	22	10.75	-	(17)
Yucca fibre	480	-	-	(18)

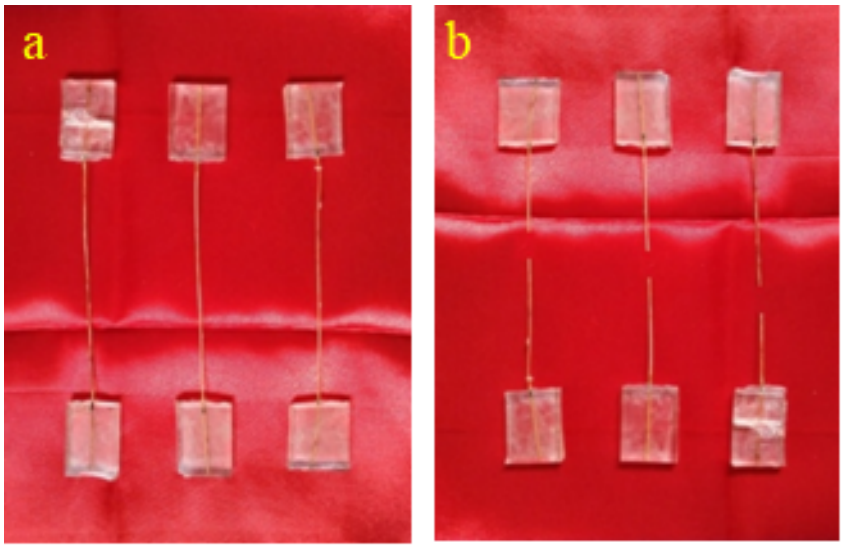

Fig 5. Samples of specimen (a) Before tensile test (b) After tensile test

3.6 Thermal Characterization

The thermal behaviour of the BPF was calculated using Thermo gravimetric analysis (TGA). Figure 6 shows a Thermogravimetry/Differential thermal analysis (DTA) plot. Thermal degradation of a natural fibre happens in the sequence of loss of moisture, hemicellulose, cellulose, lignin, wax, and the remaining constituent present, leaving residue. Three separate steps were taken to degrade the BPF ingredients. According to Figure 6, the initial degradation occurred between 100 and 268 °C. Moisture began to evaporate from the BPF at this temperature. At 494 °C, the second degradation stage degrades most cellulose and lignin content, resulting in a mass loss of approximately 85%. A shank was used to achieve maximum degradation at 794 °C and 844 °C, respectively. The final degradation stage, cellulose degradation, occurs between 494 and 982 °C, which coincide with the degradation of lignin and wax, leaving ash as a residue. Additionally, the BPFs' thermal stability is higher when compared to that of Corypha taliera fruit fibre [12]. The TGA study revealed that BPFs are a suitable substance for use as an effective reinforcement in industrial applications.

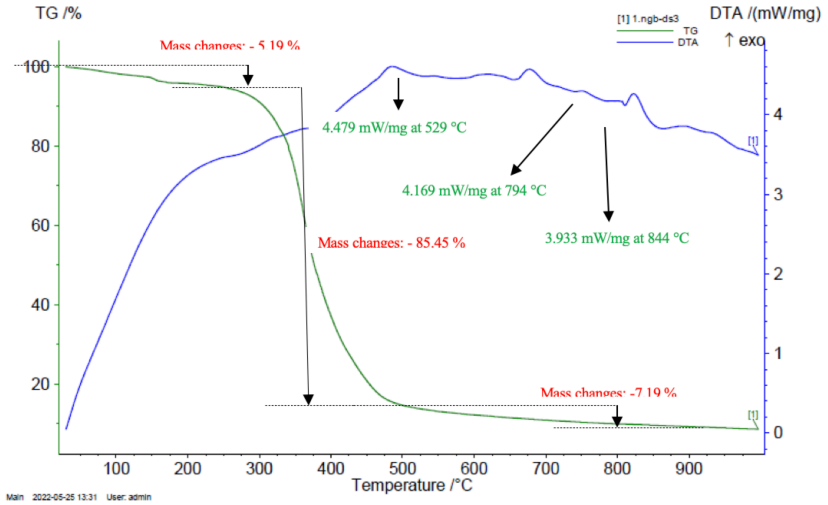

Fig 6. Thermogravimetry/Differential Thermal Analysis (TG/DTA) curve

3.7 Microstructure Analysis

Figure 7 shows the transverse and longitudinal SEM images of the BPFs to describe the morphology of the fibres. The fibre has an oval shape, as shown by the cross-sectional SEM image (Figure 7 a). BPF is composed of several primary fibres held together using pectin, which may increase the roughness of the fibre surface [19]. The cross-sectional SEM images in Figure 7 (a) show that these primary fibres exist. The longitudinal fibre section (Figure 7 (b)) shows that the surface of the fibre is not smooth and has organic compounds and other impurities. The surface of the fibre must be made so that the bond between it and the polymer matrix is strong enough. Lumen is the empty area of the primary fibre, which is seen in the cross-sectional SEM image. The fibre has strong insulation and absorption qualities due to its high lumen diameter (5 to 62 μm) [20].

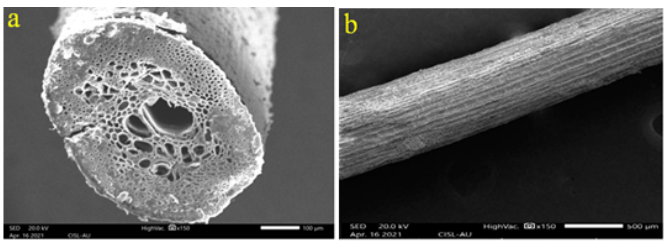

Fig 7. SEM image (a) Cross section of BPF and (b) Surface of BPF

4 Conclusion

Natural cellulose Bismarck palm fibres were extracted in this research work, and their suitability for polymer matrix composites was assessed based on their physical, chemical, mechanical, and thermal characteristics. The results of the characterization led to the following conclusions:

1. BPF had a fibre fineness of 819 deniers, a mean diameter of 0.3636 mm, and a fibre density of 0.98 g/cc (61 % lower than the glass fibre density).
2. The crystallinity index of BPF was found to be 65.93%, and the size of its crystals was found to be 5.22 nm.
3. The better mechanical properties and high thermal stability of BPF are due to its high cellulose content (70.71 %).
4. The determined mean tensile strength, Young's modulus, and percentage of breaking elongation were 904 MPa, 28.6 GPa, and 6.4 %, respectively.
5. The Thermo gravimetric analysis demonstrated the BPF's thermal stability up to 268 °C
6. The scanning electron microscopy analysis revealed that the fibre has an oval shape and rough surface, which is conducive for better interfacial strength.

The overall characteristics of these fibres indicate that they could be used as an alternative reinforcement to synthetic glass fibre in polymer matrix composite materials, which have good mechanical and thermal properties compared to the recently identified and characterised natural fibres such as Eleusine indica grass fibres, Saccharum Bengalense fibres, Leucas Aspera fibres, and Catharanthus roseus fibres. In the coming years, scientists and researchers could use the results of this study to do more research on these fibres to use as reinforcement to make valuable and long-lasting polymer composite products.

References

1) Kumar S, Manna A, Dang R. A review on applications of natural Fiber-Reinforced composites (NFRCs). *Materials Today: Proceedings*. 2022;50:1632–1636. Available from: https://doi.org/10.1016/j.matpr.2021.09.131.
2) Sathish S, Prabhu L, Gokulkumar S, Karthi N, Balaji D, Vigneshkumar N. Extraction, Treatment and Applications of Bio Fiber CompositesA Critical Review. *Composite and Composite Coatings*. 2022;36:1–22. Available from: https://doi.org/10.1201/9781003109723-1.
3) Rana P, Chopra S. Extraction and Characterization of Inherently Antimicrobial Fibres from Aerial Roots of Banyan Tree. *Journal of Natural Fibers*. 2022;19(13):6196–6213. Available from: https://doi.org/10.1080/15440478.2021.1905586.
4) Sathish S, Prabhu L, Gokulkumar S, Karthi N, Balaji D, Vigneshkumar N. Extraction, Treatment and Applications of Bio Fiber CompositesA Critical Review. *Composite and Composite Coatings*. 2022;36:1–22. Available from: https://doi.org/10.1515/ipp-2020-4004.
5) Moshi AAM, Ravindran D, Bharathi SRS, Indran S, Saravanakumar SS, Liu Y. Characterization of a new cellulosic natural fiber extracted from the root of Ficus religiosa tree. *International Journal of Biological Macromolecules*. 2020;142:212–221. Available from: https://doi.org/10.1016/j.ijbiomac.2019.09.094.
6) Raja K, Prabu B, Ganeshan P, Sekar VSC, Nagarajaganesh BS. Characterization Studies of Natural Cellulosic Fibers Extracted from Shwetark Stem. *Journal of Natural Fibers*. 2021;18(11):1934–1945. Available from: https://doi.org/10.1080/15440478.2019.1710650.
7) Vinod A, Vijay R, Singaravelu DL, Khan A, Sanjay MR, Siengchin S, et al. Effect of alkali treatment on performance characterization of Ziziphus mauritiana fiber and its epoxy composites. *Journal of Industrial Textiles*. 2022;51:2444. Available from: https://doi.org/10.1177/1528083720942614.
8) Vijay R, Vinod A, Singaravelu DL, Sanjay MR, Siengchin S. Characterization of chemical treated and untreated natural fibers from Pennisetum orientale grass- A potential reinforcement for lightweight polymeric applications. *International Journal of Lightweight Materials and Manufacture*. 2021;4(1):43–49. Available from: https://doi.org/10.1016/j.ijlmm.2020.06.008.
9) Totong T, Wardiningsih W, Al-Ayyuby M, Wanti R, Rudy R. Extraction and Characterization of Natural Fiber from Furcraea Foetida Leaves as an Alternative Material for Textile Applications. *Journal of Natural Fibers*. 2022;19(13):6044–6055. Available from: https://doi.org/10.1080/15440478.2021.1904477.
10) Asyraf MRM, Syamsir A, Supian ABM, Usman F, Ilyas RA, Nurazzi NM, et al. Sugar Palm Fibre-Reinforced Polymer Composites: Influence of Chemical Treatments on Its Mechanical Properties. *Materials*. 2022;15(11):3852. Available from: https://doi.org/10.3390/ma15113852.
11) Liu Y, Xie J, Wu N, Ma Y, Menon C, Tong J. Characterization of natural cellulose fiber from corn stalk waste subjected to different surface treatments. *Cellulose*. 2019;26(8):4707–4719. Available from: https://doi.org/10.1007/s10570-019-02429-6.
12) Tamanna TA, Belal SA, Shibly MAH, Khan AN. Characterization of a new natural fiber extracted from Corypha taliera fruit. *Scientific Reports*. 2021;11(1):1–3. Available from: https://doi.org/10.1038/s41598-021-87128-8.
13) Vijay R, Manoharan S, Arjun S, Vinod A, Singaravelu DL. Characterization of silane-treated and untreated natural fibers from stem of leucas aspera. *Journal of Natural Fibers*. 2021;18(12):1957–1973. Available from: https://doi.org/10.1080/15440478.2019.1710651.
14) Vijay R, Singaravelu DL, Vinod A, Sanjay MR, Siengchin S, Jawaid M, et al. Characterization of raw and alkali treated new natural cellulosic fibers from Tridax procumbens. *International Journal of Biological Macromolecules*. 2019;125:99–108. Available from: https://doi.org/10.1016/j.ijbiomac.2018.12.056.
15) Vijay R, Singaravelu DL, Vinod A, Raj IDFP, Sanjay MR, Siengchin S. Characterization of Novel Natural Fiber from Saccharum Bengalense Grass (Sarkanda). *Journal of Natural Fibers*. 2020;17(12):1739–1747. Available from: https://doi.org/10.1080/15440478.2019.1598914.
16) Vinod A, Vijay R, Singaravelu DL, Sanjay MR, Siengchin S, Moure MM. Characterization of untreated and alkali treated natural fibers extracted from the stem of Catharanthus roseus. *Materials Research Express*. 2019;6(8). Available from: https://doi.org/10.1088/2053-1591/ab22d9.
17) Khan A, Vijay R, Singaravelu DL, Sanjay MR, Siengchin S, Verpoort F, et al. Extraction and characterization of natural fiber from Eleusine indica grass as reinforcement of sustainable fiber reinforced polymer composites. *Journal of Natural Fibers*. 2021;18(11):1742–1750. Available from: https://doi.org/10.1080/15440478.2019.1697993.

18) Moghaddam MK, Karimi E. Structural and physical characteristics of the yucca fiber. *Journal of Industrial Textiles*. 2022;51(5_suppl):8018S–8034S. Available from: https://doi.org/10.1177/1528083720960756.
19) Keskin OY, Dalmis R, Kilic B, Seki G, Koktas Y, S. Extraction and characterization of cellulosic fiber from Centaurea solstitialis for composites. *Cellulose*. 2020;27(17):9963–9974. Available from: https://doi.org/10.1007/s10570-020-03498-8.
20) Dalmis R, Kilic GB, Seki Y, Koktas S, Keskin OY. Characterization of a novel natural cellulosic fiber extracted from the stem of Chrysanthemum morifolium. *Cellulose*. 2020;27(15):8621–8634. Available from: https://doi.org/10.1007/s10570-020-03385-2.